0026-895X/04/6506-1364–1374$20.00
MOLECULAR PHARMACOLOGY
Copyright © 2004 The American Society for Pharmacology and Experimental Therapeutics
Mol Pharmacol 65:1364–1374, 2004

Vol. 65, No. 6
3108/1151020
Printed in U.S.A.

Kv1.3-Blocking 5-Phenylalkoxypsoralens: A New Class of Immunomodulators

Julia Vennekamp, Heike Wulff, Christine Beeton, Peter A. Calabresi, Stephan Grissmer, Wolfram Hänsel, and K. George Chandy

Pharmaceutical Institute, University of Kiel, Kiel, Germany (J.V., W.H.); Department of Medical Pharmacology and Toxicology, University of California at Davis, Davis, California (H.W.); Department of Physiology and Biophysics, University of California at Irvine, Irvine, California (C.B., K.G.C.); Department of Pathology, Johns Hopkins Hospital, Baltimore, Maryland (P.A.C.); and Department of Applied Physiology, University of Ulm, Ulm, Germany (S.G.)

Received November 21, 2003; accepted February 24, 2004

This article is available online at http://molpharm.aspetjournals.org

ABSTRACT

The lymphocyte potassium channel Kv1.3 is widely regarded as a promising new target for immunosuppression. To identify a potent small-molecule Kv1.3 blocker, we synthesized a series of 5-phenylalkoxypsoralens and tested them by whole-cell patch clamp. The most potent compound of this series, 5-(4-phenylbutoxy)psoralen (Psora-4), blocked Kv1.3 in a use-dependent manner, with a Hill coefficient of 2 and an EC_{50} value of 3 nM, by preferentially binding to the C-type inactivated state of the channel. Psora-4 is the most potent small-molecule Kv1.3 blocker known. It exhibited 17- to 70-fold selectivity for Kv1.3 over closely related Kv1-family channels (Kv1.1, Kv1.2, Kv1.4, and Kv1.7) with the exception of Kv1.5 (EC_{50}, 7.7 nM) and showed no effect on human *ether-a-go-go*-related channel, Kv3.1, the calcium-activated K^+ channels (IKCa1, SK1–SK3, and BK_{Ca}), or the neuronal $Na_V1.2$ channel. In a test of in vivo toxicity in rats, Psora-4 did not display any signs of acute toxicity after five daily subcutaneous injections at 33 mg/kg body weight. Psora-4 selectively suppressed the proliferation of human and rat myelin-specific effector memory T cells with EC_{50} values of 25 and 60 nM, respectively, without persistently suppressing peripheral blood naive and central memory T cells. Because autoantigen-specific effector memory T cells contribute to the pathogenesis of T cell-mediated autoimmune diseases such as multiple sclerosis, Psora-4 and other Kv1.3 blockers may be useful as immunomodulators for the therapy of autoimmune disorders.

The voltage-gated Kv1.3 channel and the Ca^{2+}-activated IKCa1 channel promote and sustain Ca^{2+} signaling in human T cells by hyperpolarizing the membrane and providing the driving force for Ca^{2+} entry through voltage-independent Ca^{2+} channels (Lewis and Cahalan, 1995; Cahalan et al., 2001). Selective blockade of Kv1.3 and/or IKCa1 results in membrane depolarization, reduced Ca^{2+} entry, and diminished cytokine production and proliferation (DeCoursey et al., 1984; Lin et al., 1993; Ghanshani et al., 2000; Fanger et al., 2001). All quiescent human T cells express ~10-fold more Kv1.3 than IKCa1 channels (~300 Kv1.3 versus ~20 IKCa1/cell), but activation produces distinctive channel phenotypes in naive, central memory (T_{CM}) and effector memory (T_{EM}) subsets (Wulff et al., 2003b). Naive and T_{CM} cells require antigen priming in lymph nodes before trafficking to sites of inflammation, whereas T_{EM} cells rapidly enter inflamed tissues, secrete inflammatory cytokines, and exhibit immediate effector function (Sallusto et al., 1999). Mitogenic or antigenic stimulation of naive and T_{CM} cells transcriptionally augments IKCa1 expression (~500 channels/cell) while not changing Kv1.3 expression. On the other hand, T_{EM} cells up-regulate Kv1.3 but not IKCa1 during activation (~1500 versus ~20/cell). These differences dictate the effectiveness

This work was supported by grants from the National Multiple Sclerosis Society (to K.G.C., P.A.C., and C.B.), the National Institutes of Health (MH59222), the Rockefeller Brothers Fund (to K.G.C.), the American Heart Association (to H.W.), the Deutsche Forschungsgemeinschaft (Gr848/8-2; to S.G.) and the Bundesministerium für Bildung und Forschung (iZKF Ulm, B7; to S.G.).

J.V. and H.W. contributed equally to this work.

Parts of this work have been presented previously at the Meeting of the German Pharmaceutical Society in Halle [*Arch Pharm Pharm Med Chem* 2001;**334 (Suppl 2):**C72], the Experimental Biology Meeting in San Diego (*FASEB J* 2003;**17:**A1051), and in the doctoral thesis of Julia Vennekamp [Vennekamp J (2002) *Synthese und elektrophysiologische Testung hochwirksamer Psoralenderivate als nicht-peptidische Blocker des lymphozytären Kaliumkanals Kv1.3*. thesis, University of Kiel, Germany].

ABBREVIATIONS: T_{CM}, central memory T cell subset; T_{EM}, effector memory T cell subset; 5-MOP, 5-methoxysporalen; EAE, experimental autoimmune encephalomyelitis; MBP, myelin basic protein; MS, multiple sclerosis; K_v, voltage-gated K^+ channel; ShK, *Stichodactyla helianthus* toxin; HERG, human *ether-a-go-go*-related gene; HPLC, high-performance liquid chromatography; PBMC, peripheral blood mononuclear cells; [^{3}H]TdR, tritiated thymidine; WIN-17317–3, 1-benzyl-7-chloro-4-*n*-propylimino-1,4-dihydroquinoline hydrochloride; CP-339818, 1-benzyl-4-pentylimino-1,4-dihydroquinoline; UK-78282, 4-[(diphenylmethoxy)methyl]-1-[3-(4-methoxyphenyl)propyl]-piperidine.

of Kv1.3 and IKCa1 blockers in suppressing proliferation of naive/T_{CM} versus T_{EM} cells. Naive/T_{CM} cells are initially sensitive to Kv1.3 blockade but rapidly escape Kv1.3 inhibition by up-regulating IKCa1 and become sensitive to IKCa1 blockade. In contrast, Kv1.3 blockers persistently and potently suppress the proliferation of T_{EM} cells. The recent discovery that myelin-reactive T cells from patients with multiple sclerosis (MS) are Kv1.3-dependent T_{EM} cells (Wulff et al., 2003b) that arise as a consequence of repeated antigenic stimulation during the course of disease and contribute to disease pathogenesis has raised interest in developing Kv1.3 blockers for the therapy of autoimmune disorders.

Several peptide and small-molecule inhibitors of Kv1.3 have been developed over the last two decades (Chandy et al., 2001; Wulff et al., 2003a). The most potent peptide inhibitor, ShK, from the Caribbean sea anemone *Stichodactyla helianthus* (K_d, 11 pM), inhibits proliferation of T_{EM} cells with an EC_{50} of 400 pM. ShK and kaliotoxin, another Kv1.3 blocker, prevented and reversed the symptoms of experimental autoimmune encephalomyelitis (EAE), an animal model for MS, produced by the transfer of $Kv1.3^{high}$ myelin-specific rat memory cells into naive rat recipients (Beeton et al., 2001a,b). No side effects were observed. These peptides have potential therapeutic usefulness for autoimmune disorders but have to be administered parenterally, have a short circulating half-life, and their toxicity profiles remain to be determined.

Small-molecule inhibitors of Kv1.3 have chemically diverse structures. Tetraethylammonium and 4-aminopyridine with millimolar potency for the channel prevented EAE in rats at concentrations that suppressed mitogen-induced proliferation of these cells (Judge et al., 1997a,b). The first small molecules to exhibit nanomolar potency were the iminodihydroquinolines (WIN-17317–3, CP-339818) and the benzyl piperidines (UK-78282), but these were not developed further because of a lack of specificity for Kv1.3. Subsequent efforts led to the development of correolide and *trans-N*-propylcarbamoyloxy-4-phenyl-4[3-(2-methoxyphenyl)-3-oxo-2-azaprop-1-yl]cyclohexanone by Merck, dichlorophenylpyrazolopyrimidines by Bristol-Myers Squibb Co., and sulfamidebenzamidoindanes by Icagen (reviewed in Wulff et al., 2003a). None is selective and/or particularly potent for Kv1.3, necessitating a search for better blockers.

In the early 1990s, anecdotal reports from Chile and Austria suggesting that tea made from *Ruta graveolens* alleviated the symptoms of MS instigated a search for the pharmacologically active agent. Because extracts from *R. graveolens* blocked delayed-rectifier K^+ currents in nodes of Ranvier (Bohuslavizki et al., 1994), blockade of K^+ currents, either in demyelinated neurons or in myelin-reactive lymphocytes, was thought to underlie the beneficial effects of *R. graveolens*. Through extensive screening, 5-methoxypsoralen (5-MOP), a compound clinically used in the therapy of psoriasis, was identified as the major K^+ channel-blocking principle of *R. graveolens* (Bohuslavizki et al., 1994); it blocked Kv1.2 channels in neurons and Kv1.3 channels in T cells. 5-MOP reportedly improved functional deficits in MS patients (Bohuslavizki et al., 1993), but its phototoxic activity precluded its use as a therapeutic for MS. We therefore generated a nonphototoxic psoralen called H37 (Wulff et al., 1998) that suppressed cytokine secretion and proliferation of myelin-reactive encephalitogenic rat memory T cells (Strauss et al., 2000), but its micromolar affinity for Kv1.3 necessitated further analog development.

In the present study, we describe Psora-4, a 5-phenylalkoxypsoralen that preferentially binds to the C-type inactivated state of Kv1.3. Psora-4 blocks Kv1.3 with an EC_{50} value of 3 nM, making it the most potent small-molecule Kv1.3 inhibitor known. Psora-4 preferentially suppresses the proliferation of human and rat T_{EM} cells and does not cause acute toxicity when administered in vivo. Psora-4 may have use as a therapeutic in autoimmune disorders.

Materials and Methods

Chemistry. 5-MOP was purchased from Roth (Karlsruhe, Germany). 5-Hydroxypsoralen was prepared from 5-MOP through ether-cleavage with MgI_2 in anhydrous diethyl ether (Schoenberg and Aziz, 1953). The 5-phenylalkoxypsoralens (compounds 1–9 in Fig. 1) and the 5-cyclohexylalkoxypsoralens (compounds 10–12) were synthesized starting from 5-hydroxypsoralen according to the following general method: a mixture of 5-hydroxypsoralen, anhydrous K_2CO_3, a catalytic amount of KI, and the respective alkylating agent were heated to reflux in anhydrous acetone under nitrogen. After completion of the reaction, the mixture was poured into ice-cold water, acidified with HCl, and the resulting precipitate was collected by vacuum filtration and dissolved in CH_2Cl_2. This solution was washed with NaOH (2%) several times, dried over Na_2SO_4, concentrated under reduced pressure, and the residue was recrystallized. Compounds were characterized by melting point, IR, ^1H and ^{13}C NMR (for numbering, see compound 1 in Fig. 1), mass spectrometry, and combustion analysis. ^{13}C data are given only for Psora-4 (compound 4) and are available upon request for the other compounds. IR data are also available on request.

5-Benzyloxypsoralen (Compound 1). This was prepared as described previously (Caporale and Antonello, 1958).

5-(2-Phenylethoxy)psoralen (Compound 2). 5-Hydroxypsoralen (150 mg, 0.7 mmol), 2-phenylethylbromide (2.0 ml, 14.8 mmol), and K_2CO_3 (0.2 g) were heated in 10 ml of acetone for 5 h. The product was recrystallized from methanol/H_2O (80:20) as a yellowish solid (90 mg, 40%): m.p. = 154.5°C; ^1H NMR ($CDCl_3$) δ 3.18 (t, 2 H, ^3J = 6.7 Hz, 5-OCH$_2$C$\underline{H}_2$C$_6$H$_5$), 4.65 (t, 2 H, ^3J = 6.7 Hz, 5-OC$\underline{H}_2$CH$_2$C$_6$H$_5$), 6.21 (d, 1 H, ^3J = 9.8 Hz, H-3), 6.84 (dd, 1 H, ^3J = 2.4 Hz, ^5J = 0.9 Hz, H-4′), 7.14 (s, br, 1 H, H-8), 7.28 to 7.38 [m, 5 H, 5-O(CH$_2$)$_2$C$_6$$\underline{H}_5$], 7.56 (d, 1 H, ^3J = 2.4 Hz, H-5′), 7.94 (d, 1 H, ^3J = 9.8 Hz, H-4); MS m/z 306 (M^+), 106, 105 ($C_8H_9^+$), 103, 89, 79, 78, 77 ($C_6H_5^+$), 63, 51 ($C_4H_3^+$). Calculated for $C_{19}H_{14}O_4$ (306.32): C, 74.50%; H, 4.61%; O, 20.89%. Found: C, 74.43%; H 4.67%.

5-(3-Phenylpropoxy)psoralen (Compound 3). 5-Hydroxypsoralen (300 mg, 1.5 mmol), 3-phenylpropylbromide (0.3 ml, 2.0 mmol), and K_2CO_3 (0.6 g) were heated in 15 ml of acetone for 8 h. The product was recrystallized from ethanol/H_2O (80:20) as a yellowish solid (120 mg, 25%): m.p. = 109°C; ^1H NMR ($CDCl_3$) δ 2.22 (quint, 2 H, ^3J = 6.9 Hz, 5-OCH$_2$C$\underline{H}_2$CH$_2$C$_6$H$_5$), 2.88 [t, 2 H, ^3J = 7.5 Hz, 5-O(CH$_2$)$_2$C$\underline{H}_2$C$_6$H$_5$], 4.46 [t, 2 H, ^3J = 6.3 Hz, 5-OC$\underline{H}_2$(CH$_2$)$_2$C$_6$H$_5$], 6.27 (d, 1 H, ^3J = 9.8 Hz, H-3), 6.85 (dd, 1 H, ^3J = 2.2 Hz, ^5J = 0.8 Hz, H-4′), 7.13 (s, 1 H, H-8), 7.21 to 7.34 [m, 5 H, 5-O(CH$_2$)$_3$C$_6$$\underline{H}_5$], 7.55 (d, 1 H, ^3J = 2.4 Hz, H-5′), 8.10 (d, 1 H, ^3J = 9.8 Hz, H-4); MS m/z 320 (M^+), 202 (M-$C_9H_{10}^+$), 174 (202-CO^+), 119 ($C_9H_{11}^+$), 92, 91 ($C_7H_7^+$), 89, 65 ($C_5H_5^+$), 51 ($C_4H_3^+$), 41. Calculated for $C_{20}H_{16}O_4$ (320.34): C, 74.99%; H, 5.03%; O, 19.98%. Found: C, 74.20%; H, 5.14%.

5-(4-Phenylbutoxy)psoralen (Compound 4). 5-Hydroxypsoralen (300 mg, 1.5 mmol), 4-phenylbutylchloride (0.5 ml, 3.0 mmol), and K_2CO_3 (0.6 g) were heated in 15 ml of acetone for 31 h. The product was recrystallized from ethanol/H_2O (90:10) as a white solid (109 mg, 22%): m.p. = 98°C; ^1H NMR ($CDCl_3$) δ 1.86 to 1.91 [m, 4 H, 5-OCH$_2$(C$\underline{H}_2$)$_2$CH$_2$C$_6$H$_5$], 2.73 [t, 2 H, ^3J = 7.2 Hz, 5-O(CH$_2$)$_3$C$\underline{H}_2$C$_6$H$_5$], 4.44 [t, 2 H, ^3J = 6.0 Hz,

5-OC$\underline{H}_2(CH_2)_3C_6H_5$], 6.27 (d, 1 H, ^3J = 9.8 Hz, H-3), 6.89 (dd, 1 H, ^3J = 2.4 Hz, ^5J = 1.0 Hz, H-4′), 7.13 (dd, 1 H, ^5J = 0.9 Hz, ^5J = 0.7 Hz, H-8), 7.18 to 7.23 and 7.27 to 7.33 [2 m, 3 H and 2 H, 5-O$(CH_2)_4C_6\underline{H}_5$], 7.57 (d, 1 H, ^3J = 2.4 Hz, H-5′), 8.12 (dd, 1 H, ^3J = 9.8 Hz, ^5J = 0.7 Hz, H-4); ^{13}C NMR ($CDCl_3$) δ 27.70 and 29.56 [5-OCH$_2$($\underline{C}H_2$)$_2$CH$_2$C$_6$H$_5$], 35.52 [5-O$(CH_2)_3\underline{C}H_2C_6H_5$], 72.82 [5-O$\underline{C}H_2(CH_2)_3C_6H_5$], 93.95 (C-8), 105.10 (C-4′), 106.83 (C-4a), 112.62 (C-3), 113.35 (C-6), 126.03 (C-4“), 128.41 and 128.46 (C-2”,

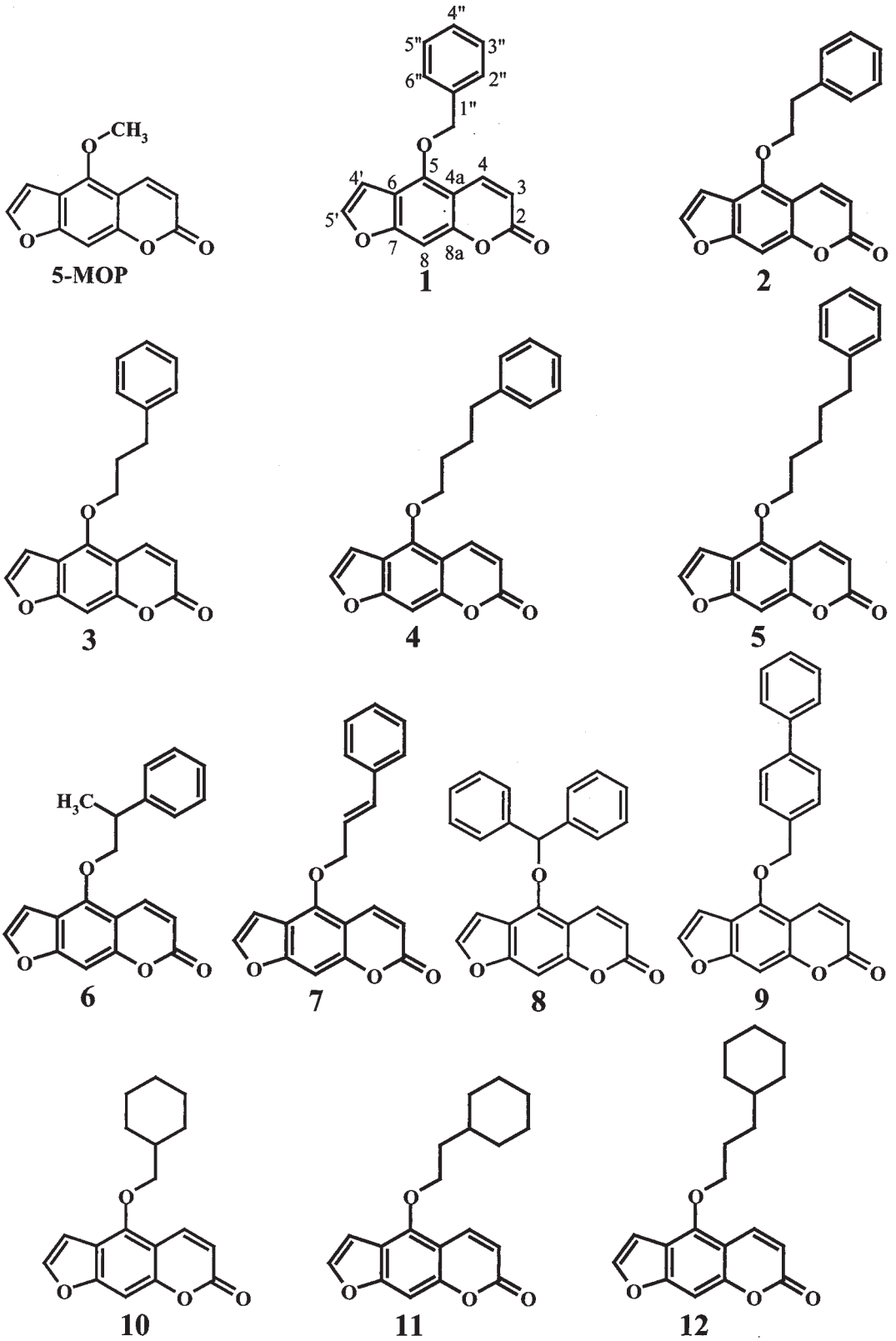

Fig. 1. Chemical structures of 5-MOP and its analogs Psora-1 through Psora-12. The numbering of the psoralen system (shown for Psora-1) is in accordance with the nomenclature most commonly used in biochemical literature.

C-3“, C-5”, C-6“), 139.31 (C-4), 141.78 (C-1”), 144.78 (C-5′), 149.01 (C-5), 152.74 (C-8a), 158.28 (C-7), 161.25 (C-2); MS *m/z* 334 (M^+), 203, 202 (M-$C_{10}H_{12}^+$), 174 (202-CO^+), 133 ($C_{10}H_{13}^+$), 92, 91 ($C_7H_7^+$), 65 ($C_5H_5^+$), 51 ($C_4H_3^+$), 44. Calculated for $C_{21}H_{18}O_4$ (334.37): C, 75.43%; H, 5.43%; O, 19.14%. Found: C, 75.34%; H, 5.41%.

5-(5-Phenylpentoxy)psoralen (Compound 5). 5-Hydroxypsoralen (300 mg, 1.5 mmol), 5-phenylpentylchloride (0.7 ml, 3.9 mmol), and K_2CO_3 (0.6 g) were heated in 15 ml of acetone for 27 h. The product was recrystallized from ethanol/H_2O (90:10) as a white solid (125 mg, 24%): m.p. = 94.5°C; ^{1}H NMR ($CDCl_3$) δ 1.53 to 1.59, 1.69 to 1.77, and 1.85 to 1.95 [3 m, 3 × 2 H, 5-OCH$_2$(C$\underline{H}_2$)$_3$CH$_2$C$_6$H$_5$], 2.67 [t, 2,H, ^3J = 7.5 Hz, 5-O(CH$_2$)$_4$C$\underline{H}_2$C$_6$H$_5$], 4.43 [t, 2 H, ^3J = 6.4 Hz, 5-OC$\underline{H}_2$(CH$_2$)$_4$C$_6$H$_5$], 6.25 (d, 1 H, ^3J = 9.8 Hz, H-3), 6.91 (dd, 1,H, ^3J = 2.4 Hz, ^5J = 1.0 Hz, H-4′), 7.12 (t, 1 H, ^5J = 0.8 Hz, H-8), 7.17 to 7.21 and 7.25 to 7.31 [2 m, 3 H and 2 H, 5-O(CH$_2$)$_4$C$_6$$\underline{H}_5$], 7.57 (d, 1 H, ^3J = 2.4 Hz, H-5′), 8.08 (dd, 1 H, ^3J = 9.8 Hz, ^5J = 0.6 Hz, H-4); MS *m/z* 348 (M^+), 203, 202 (M-$C_{11}H_{14}^+$), 174 (202-CO^+), 105, 91 ($C_7H_7^+$), 65 ($C_5H_5^+$), 51 ($C_4H_3^+$), 49, 41. Calculated for $C_{22}H_{20}O_4$ (348.40): C, 75.84%; H, 5.79%, O, 18.37%. Found: C, 75.935; H, 5.75%.

***RS*-5-(2-phenylpropoxy)psoralen (Compound 6).** 5-Hydroxypsoralen (300 mg, 1.5 mmol), β-bromocumol (0.6 ml, 3.8 mmol), and K_2CO_3 (0.6 g) were heated in 15 ml of acetone for 28 h. The product was recrystallized from ethanol/H_2O (80:20) as a yellowish solid (97 mg, 20%): m.p. = 141.5°C; ^{1}H NMR ($CDCl_3$) δ 1.47 [d, 3 H, ^3J = 7.0 Hz, 5-OCH$_2$CH(C$\underline{H}_3$)C$_6$H$_5$], 3.34 [sext, 1 H, ^3J = 7.0 Hz, 5-OCH$_2$C$\underline{H}$(CH$_3$)C$_6$H$_5$], 4.48 and 4.52 [2 dd, 2 × 1 H, $^2J_{AB}$ = 9.0 Hz, $^3J_{AX}$ = 7.0 Hz, $^3J_{BX}$ = 6.8 Hz, 5-OC$\underline{H}_A\underline{H}_BCH_X$(CH$_3$)C$_6H_5$], 6.17 (d, 1 H, ^3J = 9.8 Hz, H-3), 6.84 (dd, 1 H, ^3J = 2.4 Hz, ^5J = 0.9 Hz, H-4′), 7.13 (dd, 1 H, ^5J = 0.9 Hz, ^5J = 0.7 Hz, H-8), 7.28 to 7.39 [m, 5 H, 5-OCH$_2$CH(CH$_3$)C$_6$$\underline{H}_5$], 7.56 (d, 1 H, ^3J = 2.4, H-5′), 7.82 (dd, 1 H, ^3J = 9.8 Hz, ^5J = 0.7 Hz, H-4); MS *m/z* 320 (M^+), 203, 202 (M-$C_9H_{10}^+$), 174 (202-CO^+), 119 ($C_9H_{11}^+$), 92, 91 ($C_7H_7^+$), 77 ($C_6H_5^+$), 51 ($C_4H_3^+$), 41. Calculated for $C_{20}H_{16}O_4$ (320.34): C, 74.99%; H, 5.03%; O, 19.98%. Found: C, 74.855; H, 5.03%.

***E*-5-(3-Phenyl-2-propenyloxy)psoralen (Compound 7).** 5-Hydroxypsoralen (300 mg, 1.5 mmol), cinnamylbromide (400 mg, 2.0 mmol), and K_2CO_3 (0.6 g) were heated in 15 ml of acetone for 7 h. The product was recrystallized from ethanol/H_2O (80:20) as a yellowish solid (104 mg, 22%): m.p. = 140°C; ^{1}H NMR ($CDCl_3$) δ 5.09 (dd, 2 H, ^3J = 6.0 Hz, ^4J = 1.2 Hz, 5-OC$\underline{H}_2$CHCHC$_6$H$_5$), 6.29 (d, 1 H, ^3J = 9.8 Hz, H-3), 6.45 (dt, 1 H, ^3J = 15.9 Hz, ^3J = 6.0 Hz, 5-OCH$_2$C$\underline{H}$CHC$_6$H$_5$), 6.76 (d, br, 1 H, ^3J = 15.8 Hz, 5-OCH$_2$CHC$\underline{H}$C$_6$H$_5$), 6.98 (dd, 1 H, ^3J = 2.4 Hz, ^5J = 0.9 Hz, H-4′), 7.19 (s, br, 1 H, H-8), 7.29 to 7.43 (m, 5 H, 5-OCH$_2$CHCHC$_6$$\underline{H}_5$), 7.61 (d, 1 H, ^3J = 2.4 Hz, H-5′), 8.21 (d, 1 H, ^3J = 9.8 Hz, H-4); MS *m/z* 318 (M^+), 202 (M-$C_9H_8^+$), 174 (202-CO^+), 118, 117 ($C_9H_9^+$), 116, 115, 91 ($C_7H_7^+$), 89, 63, 51 ($C_4H_3^+$). HRMS *m/z* $C_{20}H_{14}O_4$: calculated 318.08920, found 318.08900; $C_{19}{}^{13}CH_{14}O_4$: calculated 319.09256, found 319.09240.

5-Diphenylmethoxypsoralen (Compound 8). 5-Hydroxypsoralen (200 mg, 1.0 mmol), diphenylmethylbromide (0.4 g, 1.6 mmol), and K_2CO_3 (0.4 g) were stirred at room temperature in 15 ml of acetone for 45 h. The product was recrystallized from acetone/H_2O (70:30) as a white solid (132 mg, 36%): m.p. = 173°C; ^{1}H NMR ($CDCl_3$) δ 6.29 (d, 1 H, ^3J = 9.8 Hz, H-3), 6.43 [s, 1 H, 5-OC$\underline{H}$(C$_6$H$_5$)$_2$], 6.57 (dd, 1 H, ^3J = 2.4 Hz, ^5J = 1.0 Hz, H-4′), 7.18 (t, 1 H, ^5J = 0.8 Hz, H-8), 7.30 to 7.41 [m, 10 H, 5-OCH(C$_6$$\underline{H}_5$)$_2$], 7.49 (d, 1 H, ^3J = 2.4 Hz, H-5′), 7.88 (dd, 1 H, ^3J = 9.8 Hz, ^5J = 0.6 Hz, H-4); MS *m/z* 368 (M^+), 202 (M-$C_{13}H_{10}^+$), 174 (202-CO^+), 167 ($C_{13}H_{11}^+$), 118 (174–2CO^+), 90, 89, 51 ($C_4H_3^+$), 50, 49, 44. Calculated for $C_{24}H_{16}O_4$ (368.39): C, 78.25%; H, 4.38%; O, 17.37%. Found: C, 78.175; H, 4.38%.

5-(4-Biphenylyl)methoxypsoralen (Compound 9). 5-Hydroxypsoralen (200 mg, 1.0 mmol), biphenylmethylchloride (250 mg, 1.2 mmol), and K_2CO_3 (0.4 g) were heated in 10 ml of acetone for 6 h. The product was recrystallized from acetone as a white solid (120 mg, 33%): m.p. = 187°C; ^{1}H NMR ($CDCl_3$) δ 5.49 (s, 2 H, 5-OC$\underline{H}_2$C$_6$H$_4$C$_6$H$_5$), 6.24 (d, 1 H, ^3J = 9.8 Hz, H-3), 6.97 (dd, 1 H, ^3J = 2.4 Hz, ^5J = 1.0 Hz, H-4′), 7.19 (s, br, 1 H, H-8), 7.34 to 7.66 (m, 10 H, 5-OCH$_2$C$_6$$\underline{H}_4C_6$$\underline{H}_5$ and H-5′), 8.11 (dd, 1 H, ^3J = 9.8 Hz, ^5J = 0.6 Hz, H-4); MS *m/z* 368 (M^+), 168, 167 ($C_{13}H_{11}^+$), 166, 165, 152, 145, 115, 89, 63, 51 ($C_4H_3^+$). Calculated for $C_{24}H_{16}O_4$ (368.39): C, 78.25%; H, 4.38%; O, 17.37%. Found: C, 78.285; H, 4.34%.

5-Cyclohexylmethoxypsoralen (Compound 10). 5-Hydroxypsoralen (150 mg, 0.7 mmol), cyclohexylmethylbromide (1.0 ml, 7.2 mmol), and K_2CO_3 (0.2 g) were heated in 10 ml of acetone for 23 h. The product was recrystallized from ethanol/H_2O (80:20) as a white solid (79 mg, 36%): m.p. = 153.5°C; ^{1}H NMR ($CDCl_3$) δ 1.13 to 1.38 and 1.73 to 1.94 (2 m, 5 H and 6 H, 5-OCH$_2$C$_6$$\underline{H}_{11}$), 4.24 (d, 2 H, ^3J = 5.9 Hz, 5-OC$\underline{H}_2$C$_6$H$_{11}$), 6.28 (d, 1 H, ^3J = 9.8 Hz, H-3), 6.95 (dd, 1 H, ^3J = 2.4 Hz, ^5J = 0.9 Hz, H-4′), 7.13 (s, br, 1 H, H-8), 7.57 (d, 1 H, ^3J = 2.4 Hz, H-5′), 8.17 (d, 1 H, ^3J = 9.8 Hz, H-4); MS *m/z* 298 (M^+), 203, 202 (M-$C_7H_{12}^+$), 174 (202-CO^+), 97 ($C_7H_{13}^+$), 69, 55 ($C_4H_7^+$), 51 ($C_4H_3^+$), 43, 41. Calculated for $C_{18}H_{18}O_4$ (298.34): C, 72.47%; H, 6.08%; O, 21.45%. Found: C, 72.355; H, 5.99%.

5-(2-Cyclohexylethoxy)psoralen (Compound 11). 5-Hydroxypsoralen (300 mg, 1.5 mmol), 2-cyclohexylethylbromide (0.5 ml, 3.3 mmol), and K_2CO_3 (0.6 g) were heated in 15 ml of acetone for 24 h. The product was recrystallized from ethanol/H_2O (90:10) as a white solid (263 mg, 57%): m.p. = 117°C; ^{1}H NMR ($CDCl_3$) δ 0.95 to 1.81 (m, 13 H, 5-OCH$_2$C$\underline{H}_2$C$_6$$\underline{H}_{11}$), 4.49 (t, 2 H, ^3J = 6.6 Hz, 5-OC$\underline{H}_2$CH$_2$C$_6$H$_5$), 6.28 (d, 1 H, ^3J = 9.8 Hz, H-3), 6.95 (dd, 1 H, ^3J = 2.4 Hz, ^5J = 1.0 Hz, H-4′), 7.13 (s, br, 1 H, H-8), 7,58 (d, 1 H, ^3J = 2.4 Hz, H-5′), 8.15 (dd, 1 H, ^3J = 9.8 Hz, ^5J = 0.5 Hz, H-4); MS *m/z* 312 (M^+), 203, 202 (M-$C_8H_{14}{}^+$), 174 (202-CO^+), 111 ($C_8H_{15}^+$), 69, 67, 55 ($C_4H_7^+$), 43, 41. Calculated for $C_{19}H_{20}O_4$ (312.36): C, 73.06%; H, 6.45%; O, 20.49%. Found: C, 73.115; H, 6.52%.

5-(3-Cyclohexylpropoxy)psoralen (Compound 12). 5-Hydroxypsoralen (300 mg, 1.5 mmol), 3-cyclohexylpropylchloride (0.9 ml, 5.4 mmol), and K_2CO_3 (0.6 g) were heated in 15 ml of acetone for 38 h. The product was recrystallized from ethanol/H_2O (90:10) as a white solid (223 mg, 46%): m.p. = 115°C; ^{1}H NMR ($CDCl_3$) δ 0.87 to 1.93 [m, 15 H, 5-OCH$_2$(C$\underline{H}_2$)$_2$C$_6$$\underline{H}_{11}$], 4.43 [t, 2 H, ^3J = 6.5 Hz, 5-OC$\underline{H}_2$(CH$_2$)$_2$C$_6$H$_{11}$], 6.28 (d, 1 H, ^3J = 9.8 Hz, H-3), 6.94 (dd, 1 H, ^3J = 2.4 Hz, ^5J = 1.0 Hz, H-4′), 7.13 (t, 1 H, ^5J = 0.8 Hz, H-8), 7.58 (d, 1 H, ^3J = 2.4 Hz, H-5′), 8.18 (dd, 1 H, ^3J = 9.8 Hz, ^5J = 0.6 Hz, H-4); MS *m/z* 326 (M^+), 203, 202 (M-$C_9H_{16}^+$), 174 (202-CO^+), 83, 69, 57, 55 ($C_4H_7^+$), 43, 41. Calculated for $C_{20}H_{22}O_4$ (326.39): C, 73.60%; H, 6.79%; O, 19.61%. Found: C, 73.645; H, 6.86%.

Log P Values. Log P (log of the octanol-water partition coefficient, a measure of hydrophobicity) values of compounds 1 through 12 were determined by HPLC with a Waters 1525 binary HPLC pump (Milford, MA), a Kromasil 100 C18 column (5 μm, 60 × 4.6 mm; EKA Chemicals Separation Products, Bohus, Sweden), and a Waters 2475 multiwavelength fluorescence detector. Compounds were eluted with a gradient changing from 30% acetonitrile and 70% Sörensen's phosphate buffer, 11 mM, pH 7.4 to 78% acetonitrile and 22% buffer over 70 min. 4-Methylbenzaldehyde, toluene, ethyl-, *n*-propyl-, *n*-butyl-, *n*-pentyl-, *n*-hexyl, *n*-heptyl-, and *n*-octylbenzene were used as standards.

Cells, Cell Lines, and Clones. L929, B82, and MEL cells stably expressing *mKv1.1*, *rKv1.2*, *mKv1.3*, *mKv3.1*, and *hKv1.5* have been described previously (Grissmer et al., 1994). LTK cells expressing *hKv1.4* were obtained from M. Tamkun (University of Colorado, Boulder, Boulder, CO), human embryonic kidney-293 cells expressing *hSloα* were obtained from A. Tinker (Centre for Clinical Pharmacology, University College London, London, UK), human embryonic kidney-293 cells expressing HERG (*Kv11.1*) were obtained from C. T. January (Department of Medicine, The University of Wisconsin-Madison, Madison, WI), and N1E-115 neuroblastoma cells were obtained from B. Hamprecht (Physiologisch-Chemisches Institut, Universität Tübingen, Tübingen, Germany). *hIKCa1* (*hK$_{Ca}$3.1*), *hSKCa3* (*hK$_{Ca}$2.3*), and *mKv1.7* were cloned as described previously (Wulff et al., 2000; Bardien-Kruger et al., 2002) and transiently transfected into COS-7 cells using FuGene 6 (Roche Diagnostics, Indianapolis, IN) according to the manufacturer's protocol.

The PAS T cells, a major histocompatibility complex class II-restricted MBP-specific encephalitogenic $CD4^+$ rat T cell line, were a kind gift from Dr. Evelyne Béraud (Laboratoire d'Immunologie, Faculté de Médecine, Université de la Méditerranée, Marseille, France). They were maintained in culture by alternating rounds of antigen-induced activation and expansion in interleukin-2–containing medium (Beeton et al., 2001b, 2003). Human MBP-specific $CD4^+$ memory T cells were generated from peripheral blood mononuclear cells (PBMC) from a healthy volunteer according to a split-well assay described previously (Wulff et al., 2003b). Cells were stimulated 12× with MBP and used for the proliferation assay when they were >95% $CCR7^-/CD45RA^-$ by flow cytometry.

Electrophysiology. All compounds used for electrophysiological testing were >98% pure as determined by combustion analysis. All experiments were conducted in the whole-cell configuration of the patch-clamp technique with a holding potential of −80 mV unless otherwise stated. Pipette resistances averaged 2.0 MΩ, and series resistance compensation of 80% was used when currents exceeded 2 nA. Kv1.3 currents were elicited by repeated 200-ms or 2-s pulses from −80 to 40 mV, applied at intervals of 30 or 60 s. Kv1.3 currents were recorded in normal Ringer's solution with a Ca^{2+}-free pipette solution containing 145 mM KF, 10 mM HEPES, 10 mM EGTA, and 2 mM $MgCl_2$, pH 7.2; osmolarity, 300 mOsM. EC_{50} values and Hill coefficients were determined by fitting the Hill equation to the reduction of peak current measured at 40 mV. Kv1.1, Kv1.5, Kv1.7, Kv1.4, and Kv3.1 currents were recorded with 200-ms depolarizing pulses to 40 mV applied every 10 s (Grissmer et al., 1994; Wulff et al., 2000; Bardien-Kruger et al., 2002). For Kv1.2, we applied 200-ms pulses to 40 mV every 5 s to allow for the use-dependent activation of the channel (Grissmer et al., 1994). HERG currents were recorded with a 2-step pulse from −80 mV first to 20 mV for 2 s and then to −50 mV for 2 s (Zhou et al., 1998), and the reduction of both peak and tail current by the drug was determined. For measurements of intermediate-conductance Ca^{2+}-activated K^+ channel IK_{Ca} (*$K_{Ca}3.1$*), SK_{Ca} (*$K_{Ca}2.3$*), and BK_{Ca} (*$K_{Ca}1.1$*) currents, we used an internal pipette solution containing 145 mM K^+ aspartate, 2 mM $MgCl_2$, 10 mM HEPES, 10 mM K_2EGTA, and 8.5 mM $CaCl_2$ (1 μM free Ca^{2+}), pH 7.2, 290 to 310 mOsM and an external solution containing 160 mM Na^+ aspartate, 4.5 mM KCl, 2 mM $CaCl_2$, 1 mM $MgCl_2$, and 5 mM HEPES, pH 7.4, 290 to 310 mOsM. Intermediate-conductance Ca^{2+}-activated K^+ channel and SK_{Ca} currents were elicited by 200-ms voltage ramps from −120 mV to 40 mV applied every 10 s, and the reduction of slope conductance by drug at −80 mV was taken as a measure of channel block (Wulff et al., 2000). BK_{Ca} currents were elicited by 200-ms voltage ramps from −80 to 80 mV applied every 30 s, and channel block was measured as reduction of slope conductance at 35 mV. $Na_V1.2$ currents from N1E-115 cells were recorded with 100-ms pulses from −80 to 0 mV every 10 s with a KCl-based pipette solution and an external solution containing 25 mM glucose (Hirsh and Quandt, 1996). Blockade was determined as reduction of the current minimum between 0.3 and 5 ms.

Proliferation Assays. Human PBMC were seeded at 2×10^5 cells/well in RPMI 1640 culture medium in flat-bottomed 96-well plates (final volume, 200 μl), preincubated with increasing concentrations of Psora-4 for 30 min, and then stimulated with 200 ng/ml soluble anti-CD3 monoclonal antibody (Biomeda, Foster City, CA) for 48 h. MBP-specific $CD4^+$ human memory T cells at 5×10^4 cells/well were stimulated with 200 ng/ml anti-CD3 monoclonal antibody in the presence of 5×10^4 autologous irradiated PBMC (2500 rad). PAS T cells (2×10^4 cells/well) were stimulated in the presence of 2×10^6 irradiated Lewis rat thymocytes (2500 rad) as antigen-presenting cells with 10 μg/ml MBP. [^{3}H]TdR (1 μCi/well) was added for the last 16 h. Cells were harvested onto glass fiber filters, and radioactivity was measured in a β-scintillation counter.

Results

Structure-Activity Relationship of 5-Alkoxypsoralens: Generation of a Potent Kv1.3 Blocker. Earlier structure-activity relationship studies on psoralens and related 5,7-disubstituted coumarins revealed that modifications of the psoralen system or introduction of substituents in any positions other than the 5- or the neighboring 4 or 4′ positions reduced K^+ channel-blocking activity (Wulff et al., 1998). We therefore concentrated our further synthetic efforts on the 5-position of the psoralen moiety. The structures of 5-MOP and 12 compounds in which the methyl group at the 5-position was replaced with a series of phenylalkyl or cyclohexylalkyl substituents are shown in Fig. 1. Psora-1 through Psora-5 constitute a series of phenylalkoxypsoralens in which the length of the alkyl chain linking the psoralen moiety and a side-chain phenyl ring increases from one to five CH_2 groups. Psora-6 has one methyl group in the side chain, Psora-7 has a double bond in the side chain, and Psora-8 and Psora-9 both have an additional phenyl ring in the side chain. Psora-10, -11, and -12 contain aliphatic cyclohexyl rings in place of the side-chain phenyl ring. Each compound was characterized by melting point, IR, ^{1}H and ^{13}C NMR, mass spectrometry, and combustion analysis (see *Materials and Methods*).

As an example, the effect of Psora-3 on Kv1.3 is shown in Fig. 2A. Psora-3 blocked the current in a concentration-dependent fashion, with an EC_{50} value of 6.3 nM (Fig. 2, A–C). Concentration-response curves for Psora-3 and the other members of this series (Psora-1–Psora-5) revealed that the length of the side-chain linker had a profound effect on the potencies and Hill coefficients of these compounds (Fig. 2, B and C). Increasing the length of the linker from one to four CH_2 moieties significantly enhanced potency from an EC_{50} of 350 nM for Psora-1 to an EC_{50} of 2.9 nM for Psora-4; further lengthening of the side chain reduced potency (Fig. 2, B and C). Psora-1 with one CH_2 in the side chain blocked the channel with a Hill coefficient approaching unity; whereas the other four compounds in this series, Psora-2 through Psora-5, displayed Hill coefficients of 2, suggesting that more than one inhibitor molecule interacts with one Kv1.3 channel. The biphenyl-substituted Psora-9 also blocked Kv1.3 in the single nanomolar range (EC_{50}, 3.5 nM) (Figs. 1 and 2C). Other changes in the side chain did not improve potency. Psora-6 with one methyl group in the side chain, Psora-7 with a double bond in the side chain, and Psora-8 with an additional phenyl ring were all significantly less active than Psora-3, Psora-4, Psora-5, and Psora-9. Replacement of the side-chain phenyl ring with an aliphatic cyclohexyl ring in an analogous series of compounds (Psora-10, Psora-11, and Psora-12) reduced potency.

The single nanomolar EC_{50} values of Psora-3, Psora-4, Psora-5, and Psora-9 make these four compounds the most potent known small-molecule Kv1.3 blockers; other known nonpeptide blockers of Kv1.3 have EC_{50} values greater than 50 nM (for reviews, see Chandy et al., 2001; Coghlan et al., 2001; Wulff et al., 2003a). At concentrations producing more than 50% of inhibition, blockade by these four compounds was nearly irreversible despite extensive washing. However, block by the other psoralens with lower affinities was reversible. These results indicate that this class of compounds does not covalently react with the Kv1.3 protein and that the lack

of reversibility of Psora-3, Psora-4, Psora-5, and Psora-9 is a result of their higher potency and lipophilicity.

Although the four most potent compounds are lipophilic, their potency for Kv1.3 did not correlate with their lipophilicity (Fig. 2C). The log P values (a measure of their hydrophobicity) (Hansch and Anderson, 1967; Leo, 2000) of these compounds (4.0–4.7), their molecular weights (320–360), and the number of hydrogen-bond donors and acceptors (donors 0, acceptors 4) are well within the range postulated by the Lipinksi "rule of five" (Lipinski et al., 1997) as optimal for potential drug candidates. This rule generates an "alert" for a compound indicating a possible absorption problem after oral administration if any two of the following conditions apply: molecular weight >500, log P> 5, number of hydrogen bond donors (expressed as the sum of OH and NH groups) >5, and the number of hydrogen acceptors (sum of N and O atoms) >10. Psora-4 and its analogs do not violate this rule and should therefore be orally available.

Psora-4 Binds to the Inactivated State of the Kv1.3 Channel. The most potent compound in the series, Psora-4, was studied in more detail. In the experiment shown in Fig. 3A, we applied a 200-ms depolarizing pulse to elicit a control

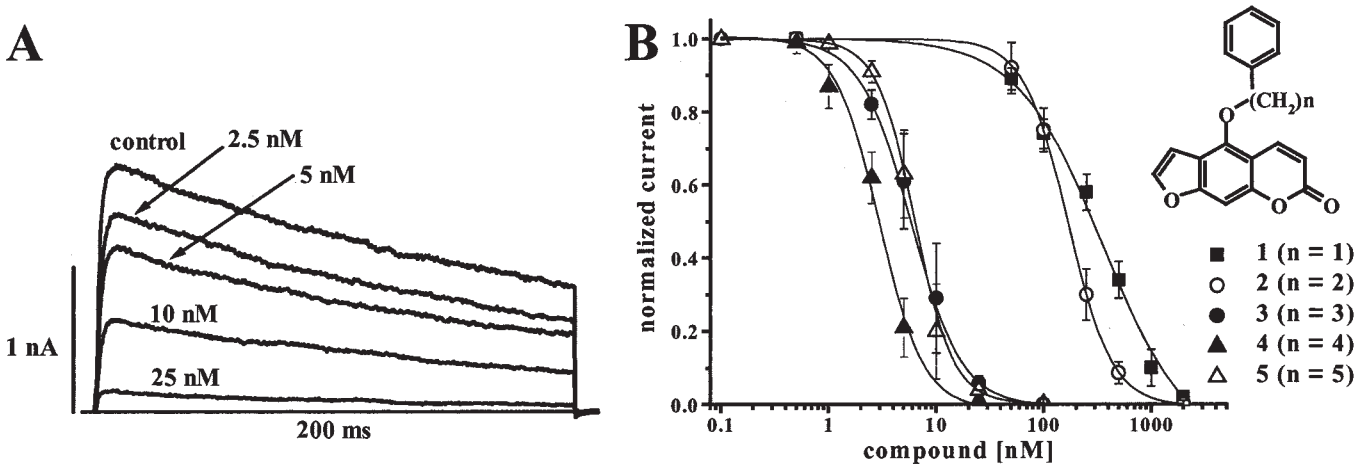

C

compound	EC_{50} Kv1.3	S	LogP
5-MOP	100 μM	14	2.15
1	350 ± 72 nM	43	3.25
2	169 ± 16 nM	41	3.55
3	6.3 ± 1.0 nM	397	3.97
4 (Psora-4)	**2.9 ± 0.3 nM**	**483**	**4.33**
5	6.1 ± 0.7 nM	262	4.71
6	172 ± 37 nM	41	3.79
7	72 ± 12 nM	25	3.87
8	68 ± 12 nM	38	4.12
9	3.5 ± 0.5 nM	286	4.40
10	138± 17 nM	48	4.41
11	132 ± 33 nM	11	4.82
12	144 ± 43 nM	8	5.34

D

Psora-4	EC_{50} [nM]
Kv1.1	62 ± 9
Kv1.2	49 ± 6
Kv1.3 (cloned)	2.9 ± 0.3
Kv1.3 (human T)	3.0 ± 0.3
Kv1.4	202 ± 12
Kv1.5	7.7 ± 0.9
Kv1.7	100 ± 12
Kv3.1	1500 ± 300
HERG	5000 ± 500
IKCa1	5000 ± 400
SKCa3	5000 ± 500
BK	5000 ± 200
Nav1.2 (N1E-115)	1400 ± 100

Fig. 2. A, inhibition of Kv1.3 current by increasing concentrations of Psora-3 in a L929 cell line stably expressing Kv1.3. For each concentration, equilibrium block after 12 pulses is shown. Currents were elicited by 200-ms depolarizing from −80 to 40 mV every 30 s. B, concentration-response curves of Psora-1, Psora-2, Psora-3, Psora-4, and Psora-5 on Kv1.3 stably expressed in L929 cells (n = number of CH_2 groups in the side chain). The compounds were tested three to five times at five or six concentrations. EC_{50} values and Hill coefficients were determined by fitting the Hill equation to the reduction of peak current measured at 40 mV. Onset of block was slow for all compounds, and equilibrium block on average was reached after 10 to 12 depolarizing pulses. The table shows EC_{50} values (mean ± S.D.), the selectivity (S) for Kv1.3 over $Na_V1.2$, and the log P values of the synthesized compounds (C). S = EC_{50} $Na_V1.2/EC_{50}$ Kv1.3. Log P values (a measure of hydrophobicity) were determined by HPLC as described under *Materials and Methods*. D, EC_{50} values of Psora-4 on cloned and native ion channels. Psora-4 was tested at three to five concentrations (n = 3). Blockade was reversible for all channels, and onset of block was slow (~10–20 depolarizing pulses to reach equilibrium block for all channels).

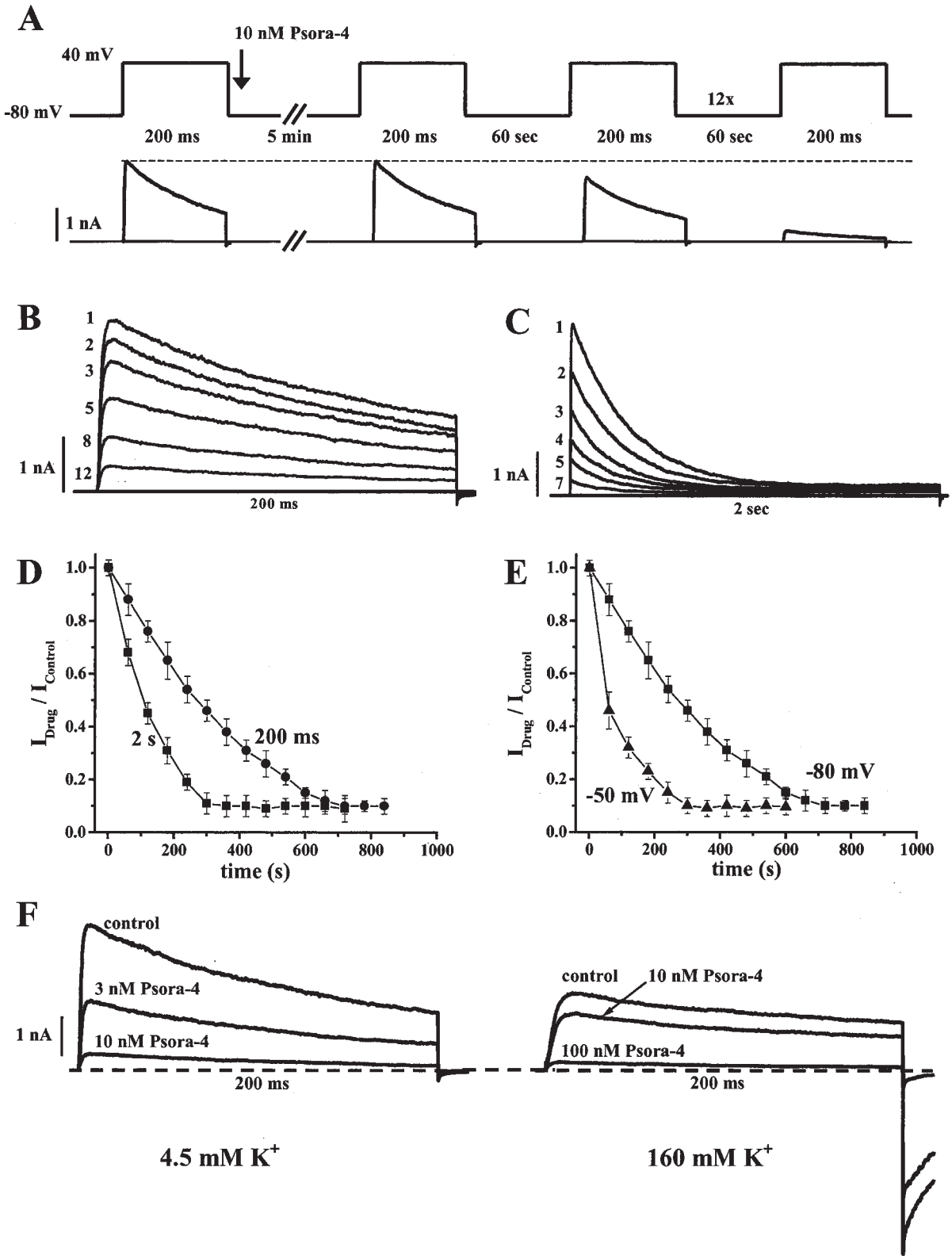

Fig. 3. A, pulse protocol for experiments shown in B–E. A Kv1.3 control current was elicited by a 200-ms depolarizing pulse to 40 mV. Psora-4 (10 nM) was then applied to the bath while the membrane was held at −80 mV. After 5 min, consecutive 200-ms or 2-s pulses were applied every 60 s. B, inhibition of Kv1.3 after application of 10 nM Psora-4 during consecutive 200-ms pulses (numbers 1–12 correspond to pulse 1–12). C, inhibition of Kv1.3 after application of 10 nM Psora-4 during consecutive 2-s pulses. D, effect of varying the pulse duration on time to reach steady-state block. Ordinate: ratio of peak current at various times after start of the consecutive pulses versus current before drug application ($n = 5$). E, effect of varying the holding potential on time to reach steady-state block. Pulse duration, 200 ms. F, effect of varying the external K^+ concentration on sensitivity to block by Psora-4. Steady-state currents 10 min after drug application (200-ms pulses to 40 mV, holding potential −80 mV) are shown. All experiments in this figure were conducted on activated T_{EM} cells because they were found to be generally more stable than L929 cells for recordings with 2-ms pulses (C and D) and for holding at depolarized potentials (E).

Kv1.3 current. Psora-4 was then perfused into the bath at a concentration (10 nM) that blocked 90% of Kv1.3 current while the channel was in the closed state. After a five-min interval to allow ample time for the lipophilic Psora-4 to reach its binding site, we applied a second depolarizing pulse and found it to be of equivalent amplitude to the control current, indicating that the compound does not bind to the closed state of the channel. Psora-4 block developed during subsequent depolarizing pulses, demonstrating that multiple openings of the channel are required to reach steady-state block, a phenomenon termed "use-dependent inhibition". This result suggests that Psora-4 blocks a postactivation state, possibly the open and/or C-type inactivated conformations of the channel.

Three types of experiments were performed to distinguish between these two possibilities. First, the time to reach steady-state block depended on the duration of the depolarizing pulse. When depolarizing pulses of 200 ms to 40 mV were applied every 60 s from a holding potential of −80 mV, 700 s was required to reach steady-state block (Fig. 3, A, B, and D). Lengthening the pulse duration to 2 s and thus causing more of the channels to undergo C-type inactivation during the pulse shortened the time to reach steady-state block to 300 s (Fig. 3, C and D). Second, the time-to-steady-state block depended on the holding potential when the pulse duration (200 ms) and the interpulse interval (60 s) were kept constant. At a holding potential of −50 mV, the proportion of channels in the C-type inactivated conformation is significantly enhanced because of prolonged recovery from inactivation compared with a more negative holding potential of −80 mV (Nguyen et al., 1996). Steady-state block was reached at ~300 s at −50 mV and at 700 s at −80 mV (Fig. 3E), consistent with Psora-4 blocking the inactivated conformation. Last, removal of C-type inactivation by 160 $[K^+]_o$ (Cahalan et al., 1985; Levy and Deutsch, 1996) decreased the potency of Psora-4 10-fold compared with 4.5 $[K^+]_o$ (Fig. 3F). Taken together, these results indicate that Psora-4 preferentially blocks the C-type inactivated conformation of the channel.

Selectivity and Lack of Toxicity of Psora-4. Psora-4 was tested for specificity against a panel of 11 channels (Fig. 2D). Psora-4 blocked cloned and native Kv1.3 channels in T cells with equivalent potency. It blocked Kv1.1, Kv1.2, Kv1.4, and Kv1.7 in a reversible fashion and displayed 16- to 70-fold selectivity for Kv1.3 over these channels. Psora-4 was ineffective against HERG (*Kv11.1*), Kv3.1, IKCa1 (*K_{Ca}3.1*), SKCa3 (*K_{Ca}2.3*), and BK_{Ca} (*K_{Ca}1.1*). Psora-3 exhibited a similar selectivity profile as Psora-4 (data not shown), whereas the more lipophilic Psora-5 and Psora-9 exhibited lower selectivity for Kv1.3 over Kv1.2 (6- and 5-fold, respectively).

The parent compound of this series, 5-MOP, blocks Na^+ channels in amphibian nodes of Ranvier at high concentrations (Bohuslavizki et al., 1994; During et al., 2000), raising concerns about possible neuronal toxicity. We therefore compared the blocking potencies of Psora-1 through Psora-9 on Kv1.3 and $Na_V1.2$, the Na^+ channel α-subunit predominantly expressed in mammalian unmyelinated and premyelinated axons (Boiko et al., 2001) (Fig. 2, C and D). Although 5-MOP was only 14-fold selective for Kv1.3 over $Na_V1.2$, Psora-3, Psora-4, and Psora-9 exhibited >300-fold selectivity for Kv1.3 over $Na_V1.2$; blockade by these compounds was completely reversible. The cyclohexyl-substituted compounds showed significantly reduced selectivity for Kv1.3 over $Na_V1.2$ (Fig. 2C).

Besides Kv1.3, the only other channel blocked potently by Psora-4 was Kv1.5 (EC_{50}, 7.7 nM), which is thought to underlie the ultrarapid delayed rectifier (IK_{UR}) current in the human atrium (Feng et al., 1997) and to contribute to atrial repolarization (Wang et al., 1993). Psora-3 (EC_{50}, 24 ± 2 nM) and Psora-9 (EC_{50}, 8.2 ± 0.5 nM) also potently blocked this channel. Interestingly, Psora-4 is 50-fold more potent as a blocker of Kv1.5 than the bisaryl S9947, a compound identified recently by Aventis (Bachmann et al., 2001). Because of concerns about possible cardiac side effects, we injected rats with Psora-4 subcutaneously (33 mg/kg/day for 5 days); the rats (n = 8) seemed clinically normal (no signs of discomfort, seizures, paralysis, ataxia, or weakness) during the 5-day study and for 7 days afterward. The lack of overt toxicity in vivo encouraged us to evaluate Psora-4 further as an immunosuppressive.

Psora-4 Preferentially Suppresses the Proliferation of T_{EM} Cells. We compared the ability of Psora-4 to suppress mitogen- or antigen-stimulated increases in [^{3}H]thymidine incorporation by a mixture of naive and T_{CM} cells versus a population of T_{EM} cells. Human T cells (either the naive/T_{CM} mixed population or MBP-specific T_{EM} cells) were stimulated through the T-cell receptor with a mitogenic monoclonal anti-CD3 antibody and myelin-specific rat T_{EM} cells with the antigen MBP in the presence or absence of Psora-4. The numbers of Kv1.3 and IKCa1 channels expressed per cell in resting and activated naive, T_{CM}, and T_{EM} subsets is shown in Fig. 4A based on data published previously (Wulff et al., 2003b). The proliferation of human and rat T_{EM} cells was suppressed by Psora-4 with EC_{50} values of 25 and 60 nM, respectively (Fig. 4B, graph top right), in keeping with the Kv1.3 dependence of these cells. Psora-4 was 10-fold less effective in suppressing the proliferation of naive/T_{CM} cells (EC_{50}, 600 nM) presumably because they quickly up-regulated IKCa1 and escaped Psora-4 inhibition (Fig. 4B, graph top left). Consistent with this idea, naive/T_{CM} cells that had been activated for 48 h to up-regulate IKCa1, rested for 12 h, and then rechallenged for a further 48 h were completely resistant to Psora-4 and sensitive to the IKCa1-specific inhibitor TRAM-34 (Fig. 4B, graph bottom left). Thus, T_{EM} cells are highly sensitive to suppression by Psora-4 because they up-regulate Kv1.3 and not IKCa1 during activation (Fig. 4A). Naive and T_{CM} cells, in contrast, are initially ~10-fold less sensitive to Psora-4 than T_{EM} cells and then become resistant to Kv1.3 blockade via up-regulation of IKCa1. These results corroborate our recent findings with the Kv1.3-blocking peptide ShK (Wulff et al., 2003b) and demonstrate that Psora-4 might have value as a potential new therapeutic for autoimmune diseases dominated by autoreactive T_{EM} cells.

Discussion

Using 5-MOP as a template, we have developed a series of 5-phenyl-alkoxypsoralens that inhibit Kv1.3 with single nanomolar affinity. The pharmacophore for channel block consists of a psoralen moiety that is attached through an alkyl chain linker in the 5-position to a phenyl ring. The optimal length for the linker was found to be four CH_2 groups as in Psora-4, our most potent compound (EC_{50}, 3 nM). Re-

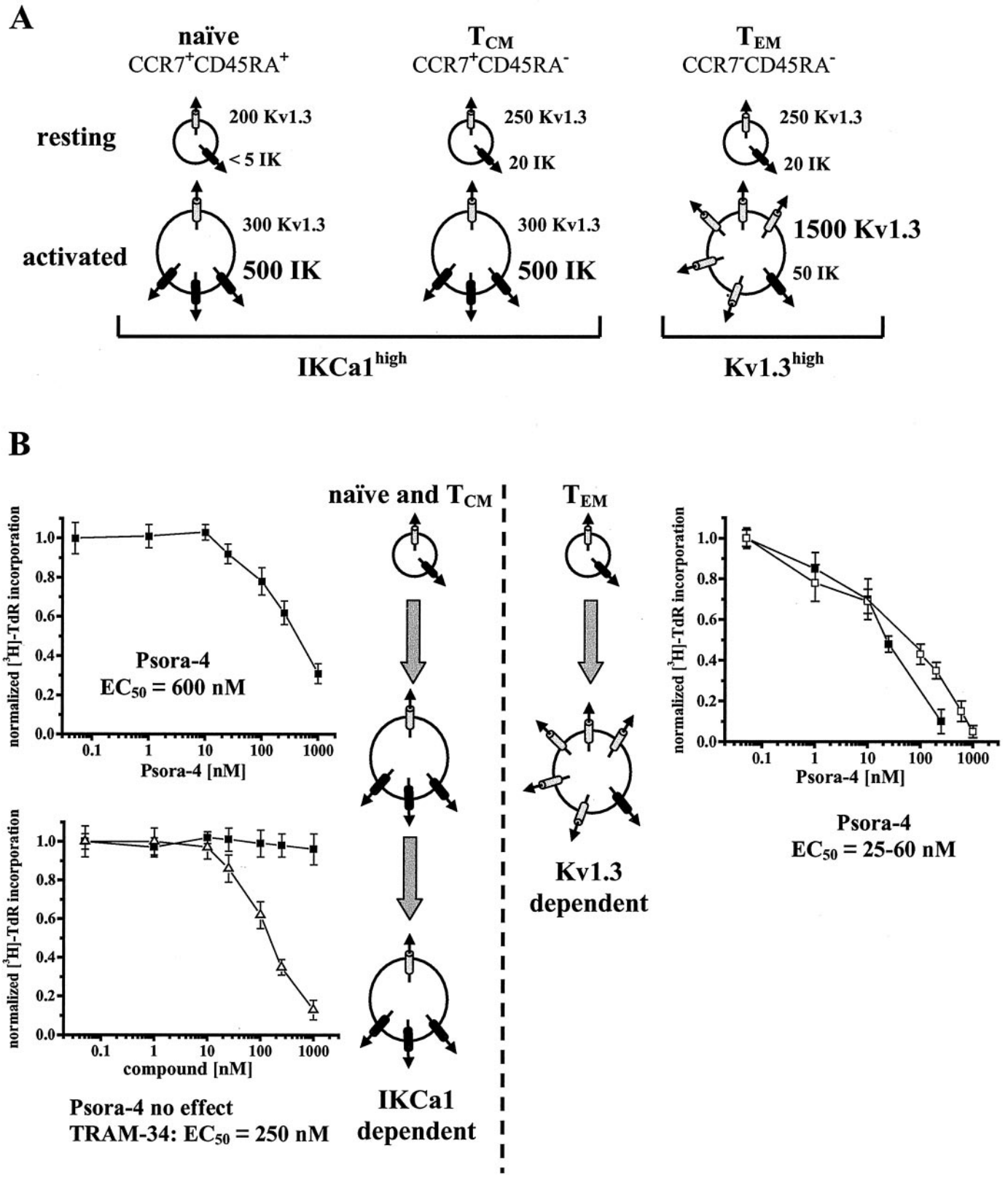

Fig. 4. A, diagram showing Kv1.3 and IKCa1 channel numbers per cell in human naive, T_{CM}, and T_{EM} T cells in the resting and activated state based on our data published previously (Wulff et al., 2003b). B, effect of Psora-4 on the proliferation of different T cell subsets. Top left, Psora-4 (■) inhibits the anti-CD3 antibody-stimulated proliferation of human peripheral blood T cells, consisting mostly of naive and T_{CM} cells, with an EC_{50} of 600 nM. Bottom left, the proliferation of prestimulated naive and T_{CM} cells is inhibited by the IKCa1 blocker TRAM-34 (△) with an EC_{50} of 250 nM but not by Psora-4 (■). Top right, the anti-CD3 antibody-stimulated proliferation of human T_{EM} cells (■) and the MBP-stimulated proliferation of rat memory T cells (□) is inhibited by Psora-4 with EC_{50} values of 25 and 60 nM, respectively.

placement of the phenyl ring with an aliphatic cyclohexyl ring (e.g., Psora-10–Psora-12) reduced Kv1.3-blocking potency and selectivity over Na^+ channels, suggesting that the phenyl ring represents a second center of π-electron density in these compounds and is required for the selective and high-affinity interaction with Kv1.3. From these structure-activity relationships, we postulate that the 5-phenylalkoxypsoralens bind to Kv1.3 via two π-π electron interactions positioned ~7 Å apart (the length of the butoxy linker in Psora-4), one involving the psoralen moiety and the second involving the side chain of the phenyl ring. The precise binding site of Psora-4 on the Kv1.3 channel remains to be determined.

Psora-4, the most potent small-molecule Kv1.3 blocker known, blocks the channel in a use-dependent manner by binding to the C-type inactivated state in a fashion similar to the other Kv1.3 blockers, including CP-339818 (Nguyen et al., 1996), UK-78282 (Hanson et al., 1999), and correolide (Hanner et al., 1999). In contrast to Psora-4, most known peptide and small-molecule Kv1.3 blockers have Hill coefficients of 1, consistent with a 1:1 stoichiometry of interaction between blocker and channel protein (Nguyen et al., 1996; Hanner et al., 1999; Hanson et al., 1999; Chandy et al., 2001). The Hill coefficient of 2 observed for Psora-4 and its analogs suggests that two molecules of blocker interact with one Kv1.3 channel tetramer, as has been reported recently for PAC and its derivatives (Schmalhofer et al., 2002, 2003). Psora-4 has a log P value of 4.33, well in the range for a therapeutic, exhibits 16- to 70-fold selectivity for Kv1.3 over closely related Kv1 channels, and does not affect other K^+ channels (HERG, BK_{Ca}, IKCa1, and SKCa3) or the neuronal sodium channel $Na_V1.2$. However, Psora-4 blocks Kv1.5 (EC_{50}, 7.7 nM), the ultrarapid delayed rectifier (IK_{UR}) current in the human atrium (Fedida et al., 1993; Feng et al., 1997), raising concerns about possible acute cardiac toxicity. Despite potently blocking Kv1.5, Psora-4 did not display any signs of acute toxicity when administered to rats at 33 mg/kg for 5 days or by a single intravenous bolus. More extensive toxicity studies will have to be performed to discern whether Psora-4 is indeed safe for in vivo use as an immunomodulator.

In keeping with the functional dependence of T_{EM} cells on Kv1.3 (Beeton et al., 2001b; Wulff et al., 2003b), Psora-4 potently suppressed the proliferation of human and rat T_{EM} cells but had little effect on naive and T_{CM} cells, which depend on IKCa1 for their activation process. Autoreactive T cells from patients with MS (Lovett-Racke et al., 1998; Scholz et al., 1998; Markovic-Plese et al., 2001) and type-1 diabetes (Viglietta et al., 2002) have been reported previously to be predominantly memory cells. Our recent studies in MS indicate that the majority of these autoreactive memory cells exhibit the $Kv1.3^{high}$ T_{EM} phenotype (Beeton et al., 2001b; Wulff et al., 2003b) and may contribute to disease pathogenesis by virtue of their ability to migrate to sites of inflammation and contribute to the inflammatory process via the secretion of cytokines. By suppressing cytokine production and proliferation of these autoreactive memory cells, Psora-4 might stop the progression of MS and other T cell-mediated autoimmune disorders. Such a Kv1.3-based therapy would have advantage over generalized immunomodulators, because naive/T_{CM} cells would escape inhibition through up-regulation of IKCa1, leaving the bulk of the immune response unimpaired. Future studies will have to be performed to ascertain whether Psora-4 is therapeutically effective in chronic relapsing models of EAE that resemble human MS more closely than monophasic adoptive-transfer EAE and whether this compound, if appropriately formulated for oral administration, will benefit patients with MS.

Acknowledgments

We thank Professor Dr. Eilhard Koppenhöfer for his courage in investigating the effects of *R. graveolens* and his continuing enthusiastic belief in psoralens as possible drugs for the treatment of MS. We also thank Björn Henke for excellent technical assistance with the chemical synthesis and Susann Häuer and Inga Carstens for their determination of the log P values.

References

Bachmann A, Gutcher I, Kopp K, Brendel J, Bosch RF, Busch AE, and Gogelein H (2001) Characterization of a novel Kv1.5 channel blocker in Xenopus oocytes, CHO cells, human and rat cardiomyocytes. *Naunyn-Schmiedeberg's Arch Pharmacol* **364:**472–478.

Bardien-Kruger S, Wulff H, Arieff Z, Brink P, Chandy KG, and Corfield V (2002) Characterization of the human voltage-gated potassium channel gene, KCNA7, a candidate gene for inherited cardiac disorders and its exclusion as a cause of progressive familial heart block I (PFHBI). *Eur J Human Gen* **10:**36–43.

Beeton C, Barbaria J, Giraud P, Devaux J, Benoliel A, Gola M, Sabatier J, Bernard D, Crest M, and Beraud E (2001a) Selective blocking of voltage-gated K^+ channels improves experimental autoimmune encephalomyelitis and inhibits T cell activation. *J Immunol* **166:**936–944.

Beeton C, Wulff H, Barbaria J, Clot-Faybesse O, Pennington M, Bernard D, Cahalan MD, Chandy KG, and Beraud E (2001b) Selective blockade of T lymphocyte K^+ channels ameliorates experimental autoimmune encephalomyelitis, a model for multiple sclerosis. *Proc Natl Acad Sci USA* **98:**13942–13947.

Beeton C, Wulff H, Singh S, Bosko S, Crossley G, Gutman GA, Cahalan MD, Pennington M, and Chandy KG (2003) A novel fluorescent toxin to detect and investigate Kv1.3-channel up-regulation in chronically activated T lymphocytes. *J Biol Chem* **278:**9928–9937.

Bohuslavizki KH, Hansel W, Kneip A, Koppenhofer E, Niemoller E, and Sanmann K (1994) Mode of action of psoralens, benzofurans, acridones and coumarins on the ionic currents in intact myelinated nerve fibres and its significance in demyelinating diseases. *Gen Physiol Biophys* **13:**309–328.

Bohuslavizki KH, Hinck-Kneip C, Kneip A, Koppenhöfer E, and Reimers A (1993) Reduction of MS-related scotoma by a new class of potassium channel blockers from Ruta graveolens. *Neuroopthalmology* **13:**191–198.

Boiko T, Rasband MN, Levinson SR, Caldwell JH, Mandel G, Trimmer JS, and Matthews G (2001) Compact myelin dictates the differential targeting of two sodium channel isoforms in the same axon. *Neuron* **30:**91–104.

Cahalan MD, Chandy KG, DeCoursey TE, and Gupta S (1985) A voltage-gated potassium channel in human T lymphocytes. *J Physiol (Lond)* **358:**197–237.

Cahalan MD, Wulff H, and Chandy KG (2001) Molecular properties and physiological roles of ion channels in the immune system. *J Clin Immunol* **21:**235–252.

Caporale G and Antonello C (1958) Sintesi di alcuni derivati furocumarinici. *Il Farmaco Ed Sci* **13:**363–367.

Chandy KG, Cahalan MD, Pennington M, Norton RS, Wulff H, and Gutman GA (2001) Potassium channels in T lymphocytes: toxins to therapeutic immunosuppressants. *Toxicon* **39:**1269–1276.

Coghlan MJ, Carrol WA, and Gopalakrishnan M (2001) Recent developments in the biology and medicinal chemistry of potassium channel modulators: update from a decade of progress. *J Med Chem* **44:**1–27.

DeCoursey TE, Chandy KG, Gupta S, and Cahalan MD (1984) Voltage-gated K^+ channels in human T lymphocytes: a role in mitogenesis? *Nature (Lond)* **307:**465–468.

During T, Gerst F, Hänsel W, Wulff H, and Koppenhöfer E (2000) Effects of three alkoxypsoralens on voltage gated ion channels in Ranvier nodes. *Gen Physiol Biophys* **19:**345–364.

Fanger CM, Rauer H, Neben AL, Miller MJ, Rauer H, Wulff H, Rosa JC, Ganellin CR, Chandy KG, and Cahalan MD (2001) Calcium-activated potassium channels sustain calcium signaling in T lymphocytes. *J Biol Chem* **276:**12249–12256.

Fedida D, Wible B, Wang Z, Fermini B, Faust F, Nattel S, and Brown A (1993) Identity of a novel delayed rectifier current from human heart with a cloned K^+ channel current. *Circ Res* **73:**210–216.

Feng J, Wible B, Li GR, Wang Z, and Nattel S (1997) Antisense oligodeoxynucleotides directed against Kv1.5 mRNA specifically inhibit ultrarapid delayed rectifier K^+ current in cultured adult human atrial myocytes. *Circ Res* **80:**572–579.

Ghanshani S, Wulff H, Miller MJ, Rohm H, Neben A, Gutman GA, Cahalan MD, and Chandy KG (2000) Up-regulation of the IKCa1 potassium channel during T-cell activation: molecular mechanism and functional consequences. *J Biol Chem* **275:**37137–37149.

Grissmer S, Nguyen AN, Aiyar J, Hanson DC, Mather RJ, Gutman GA, Karmilowicz MJ, Auperin DD, and Chandy KG (1994) Pharmacological characterization of five cloned voltage-gated K^+ channels, types Kv1.1, 1.2, 1.3, 1.5, and 3.1, stably expressed in mammalian cell lines. *Mol Pharmacol* **45:**1227–1234.

Hanner M, Schmalhofer WA, Green B, Bordallo C, Liu J, Slaughter RS, Kaczorowski GJ, and Garcia ML (1999) Binding of correolide to Kv1 family potassium channels. *J Biol Chem* **274:**25237–25244.

Hansch C and Anderson SM (1967) The effect of intramolecular hydrophobic bonding on partition coefficients. *J Org Chem* **32:**2583–2586.

Hanson DC, Nguyen A, Mather RJ, Rauer H, Koch K, Burgess LE, Rizzi JP, Donovan CB, Bruns MJ, Canniff PC, et al. (1999) UK-78,282, a novel piperidine compound that potently blocks the Kv1.3 voltage-gated potassium channel and inhibits human T cell activation. *Br J Pharmacol* **126:**1707–1716.

Hirsh JK and Quandt FN (1996) Down-regulation of Na channel expression by A23187 in N1E-115 neuroblastoma cells. *Brain Res* **706:**343–346.

Judge SIV, Paterson PY, Mannie MD, and Yeh JZ (1997a) Modulation of outward K^+ conductance is a post-activational event in rat T lymphocytes responsible for the adoptive transfer of experimental allergic encephalomyelitis. *J Biomed Sci* **4:**98–110.

Judge SIV, Yeh ZJ, Mannie MD, Seifert LP, and Paterson PY (1997b) Potassium channel blockers inhibit adoptive transfer of experimental allergic encephalomyelitis by myelin-basic protein stimulated rat T lymphocytes. *J Biomed Sci* **4:**169–178.

Leo A (2000) Octanol/water partition coefficients, in *Handbook of Property Estimation Methods for Chemicals* (Boethling RS and Mackay D eds) pp 89–114, Lewis Publishers, Boca Raton, FL.

Levy DI and Deutsch C (1996) Recovery from C-type inactivation is modulated by extracellular potassium. *Biophys J* **70:**798–805.

Lewis RS and Cahalan MD (1995) Potassium and calcium channels in lymphocytes. *Annu Rev Immunol* **13:**623–653.

Lin CS, Boltz RC, Blake JT, Nguyen M, Talento A, Fischer PA, Springer MS, Sigal NH, Slaughter RS, Garcia ML, et al. (1993) Voltage-gated potassium channels regulate calcium-dependent pathways involved in human T lymphocyte activation. *J Exp Med* **177:**637–645.

Lipinski CA, Lombardo F, Dominy BW, and Feeney PJ (1997) Experimental and computational approaches to estimate solubility and permeability in drug discovery and development settings. *Adv Drug Delivery Rev* **23:**3–25.

Lovett-Racke AE, Trotter JL, Lauber J, Perrin PJ, June CH, and Racke MK (1998) Decreased dependence of myelin basic protein-reactive T cells on CD28-mediated costimulation in multiple sclerosis patients: a marker of activated/memory T cells. *J Clin Investig* **101:**725–730.

Markovic-Plese S, Cortese I, Wandinger KP, McFarland HF, and Martin R (2001) $CD4^+CD28^-$ costimulation-independent T cells in multiple sclerosis. *J Clin Investig* **108:**1185–1194.

Nguyen A, Kath JC, Hanson DC, Biggers MS, Canniff PC, Donovan CB, Mather RJ, Bruns MJ, Rauer H, Aiyar J, et al. (1996) Novel nonpeptide agents potently block the C-type inactivated conformation of Kv1.3 and suppress T cell activation. *Mol Pharmacol* **50:**1672–1679.

Sallusto F, Lenig D, Forster R, Lipp M, and Lanzavecchia A (1999) Two subsets of memory T lymphocytes with distinct homing potentials and effector functions. *Nature (Lond)* **401:**708–712.

Schmalhofer WA, Bao J, McManus OB, Green B, Matyskiela M, Wunderler D, Bugianesi RM, Felix JP, Hanner M, Linde-Arias A-R, et al. (2002) Identification of a new class of inhibitors of the voltage-gated potassium channel, Kv1.3, with immunosuppressant properties. *Biochemistry* **18:**7781–7794.

Schmalhofer WA, Slaughter RS, Matyskiela M, Felix JP, Tang YS, Rupprecht K, Kaczorowski GJ, and Garcia ML (2003) Di-substituted cyclohexyl derivatives bind to two identical sites with positive cooperativity on the voltage-gated potassium channel Kv1.3. *Biochemistry* **42:**4733–4743.

Schoenberg A and Aziz G (1953) Furochromones and coumarins. VI. Demethylation of xantotoxin, khellin and khellol with aniline hydrochloride and magnesium iodide. *J Am Chem Soc* **75:**3265–3266.

Scholz C, Anderson DE, Freeman GJ, and Hafler DA (1998) Expansion of autoreactive T cells in multiple sclerosis is independent of exogenous B7 costimulation. *J Immunol* **160:**1532–1538.

Strauss U, Wissel K, Jung S, Wulff H, Haensel W, Zhu J, Rolfs A, and Mix E (2000) K^+ channel blocking alkoxypsoralens inhibit the immune response of encephalitogenic T line cells and lymphocytes from Lewis rats challenged for experimental autoimmune encephalomyelitis. *Immunopharmacology* **48:**51–63.

Viglietta V, Kent SC, Orban T, and Hafler DA (2002) GAD65-reactive T cells are activated in patients with autoimmune type 1a diabetes. *J Clin Investig* **109:**895–903.

Wang Z, Fermini B, and Nattel S (1993) Sustained depolarization-induced outward current in human atrial myocytes: evidence for a novel delayed rectifier K^+ current similar to Kv1.5 cloned channel currents. *Circ Res* **73:**1061–1076.

Wulff H, Beeton C, and Chandy KG (2003a) Potassium channels as therapeutic targets for autoimmune disorders. *Curr Opin Drug Discov Dev* **6:**640–647.

Wulff H, Calabresi PA, Allie R, Yun S, Pennington M, Beeton C, and Chandy KG (2003b) The voltage-gated Kv1.3 K^+ channel in effector memory T cells as new target for MS. *J Clin Investig* **111:**1703–1713.

Wulff H, Miller MJ, Hänsel W, Grissmer S, Cahalan MD, and Chandy KG (2000) Design of a potent and selective inhibitor of the intermediate-conductance Ca^{2+}-activated K^+ channel, IKCa1: a potential immunosuppressant. *Proc Natl Acad Sci USA* **97:**8151–8156.

Wulff H, Rauer H, During T, Hanselmann C, Ruff K, Wrisch A, Grissmer S, and Hansel W (1998) Alkoxypsoralens, novel nonpeptide blockers of Shaker-type K^+ channels: synthesis and photoreactivity. *J Med Chem* **41:**4542–4549.

Zhou Z, Gong Q, Ye B, Fan Z, Makielski JC, Robertson GA, and January CT (1998) Properties of HERG channels stably expressed in HEK 293 cells studied at physiological temperatures. *Biophys J* **74:**230–241.

Address correspondence to: K. George Chandy, Department of Physiology and Biophysics, Medical School, 346-D Med. Sci. I, University of California at Irvine, Irvine, CA 92697. E-mail: gchandy@uci.edu